Automotive Experiences
Vol. 7 No. 2 (2024) pp. 321-332
p-ISSN: 2615-6202 e-ISSN: 2615-6636

Research Paper

Combustion Analysis of Ammonia/Gasoline Mixtures at Various Injection Timing Conditions in a High Compression Ratio SI Engine with Sub-Chamber

Mitsuhisa Ichiyanagi[1], Emir Yilmaz[1], Takashi Suzuki[1], Takanobu Okada[2], Hikaru Yamamoto[2], Masashi Kodaka[2], Hikaru Shiraishi[2], Shinnosuke Mukae[1], Ryota Tamba[1], Henry Widjaja[3], Leon Jonathan[3], Sebastian Gunawan[3], Gabriel J. Gotama[4], Willyanto Anggono[3,4]

[1]Department of Engineering and Applied Sciences, Faculty of Science and Technology, Sophia University, Tokyo 102-8554, Japan
[2]Graduate School of Science and Technology, Sophia University, Tokyo 102-8554, Japan
[3]Department of Mechanical Engineering, Petra Christian University, Surabaya 60236, Indonesia
[4]Centre for Sustainable Energy Studies, Petra Christian University, Surabaya 60236, Indonesia

willy@petra.ac.id

https://doi.org/10.31603/ae.10533

Published by Automotive Laboratory of Universitas Muhammadiyah Magelang

Article Info
Submitted: 14/11/2023
Revised: 15/03/2024
Accepted: 17/03/2024
Online first: 18/09/2024

Abstract

Due to the problem with carbon dioxide (CO_2) emissions, alternative fuels such as ammonia (NH_3) have been garnering a lot of attention lately. This is due to its carbon-free molecular structure, ease of transport, and high energy density. Unfortunately, ammonia is not without flaws since it is considered a difficult fuel to burn in conventional internal combustion engines. To further investigate the burning characteristics of ammonia, this study is conducted for ammonia/gasoline co-combustion using a modified engine equipped with a sub-chamber. The engine ran at 1000 RPM and had a 17.7 compression ratio with two injection timings of -55° and 10° crank angle (CA) after the top dead center (ATDC), while the ammonia energy ratios were adjusted across a range from 40% to 70%. The results show that the earlier injection timing allowed better premixing between the air and fuel mixture, thus enhancing the overall combustion characteristics. For the later injection timing, the nitrogen oxides (NOx) emissions decrease at the higher ammonia energy ratio due to the denitrification of nitrogen oxides (DeNOX) process. Overall, the earlier injection timing appears to be optimal for 40% to 70% ammonia energy ratio under the present condition.

Keywords: Alternative fuels; Ammonia; Co-combustion; Sub-chamber; Injection timing

1. Introduction

Global warming is an issue that indiscriminately affects everyone on the planet. According to the Environmental Protection Agency (EPA), the major donors of greenhouse gasses are carbon dioxide (CO_2) emissions, which account for 65% of the total GHG emission [1]. The staggering amount of CO_2 emissions is primarily due to oil and other fossil fuels being the world's primary energy source, especially for the transportation sector [2]. The predominant approach to curbing carbon emissions is by transitioning to electric vehicles. However, these vehicles still face challenges arising from limitations in battery technology, infrastructural deficiencies, and limited power output [3]–[5]. Thus, a conventional combustion method based on carbon-free fuels still has a lot to offer as a solution to global warming.

Alternative fuels, such as hydrogen [6], biofuel [7], [8], pyrolysis oil [9], and ammonia [10], have been investigated in some previous studies as

alternative energy sources. Among them, hydrogen is particularly attractive because its combustion only produces water. However, the high transportation and storage costs still limit its popularity [11], [12]. Conversely, ammonia serves as another carbon-free fuel option. The study done by Koike et al [13], implies that liquid ammonia can be transported more effectively when compared to hydrogen.

Despite its benefits, using ammonia as engine fuel still has its shortcomings, including high ignition energy [14], low laminar burning velocity [10], [15], [16], toxicity [17], corrosion to copper alloys [18], and NO_x emissions. To overcome these shortcomings, there was a significant amount of research dedicated to enhancing the performance of ammonia fuel in an IC engine. Blending ammonia with a highly reactive fuel is a commonly employed technique to enhance the combustibility of ammonia. Previous studies have successfully blended ammonia with gasoline [19] and other fuels [20]–[23]. Moreover, several previous studies have also succeeded in improving ammonia combustibility by implementing a sub-chamber in a spark ignition engine and combustion chamber [19], [24], [25]. Furthermore, there have been successful experiments running on pure ammonia at very low loads using a spark-assisted compression ignition engine with high compression ratio [26]. Trung and Tuan did an experiment on the effect of port injection with ethanol and diesel which showed that earlier injection timing resulted in higher in-cylinder pressure [27]. However, the effect of ammonia injection timing is not widely studied, especially with the port injection method in a co-combustion engine.

In line with previous studies, the authors decided to use a spark-assisted compression ignition (SACI) engine with a sub-chamber and a high compression ratio using a NH_3/gasoline mixture as fuel. The goal of this study was to examine the impact of early and late injection timing across 40% to 70% ammonia energy ratio while maintaining stable NH_3/gasoline co-combustion.

2. Experimental Methods

2.1. Experimental Setup

A modified YANMAR TF120V diesel engine was used for this experiment due to its high compression ratio, which is adapted from a previous experiment [19]. **Table 1** provides the engine specifications and **Figure 1** illustrates the schematic view of the experiment setup. The engine consists of a sub-chamber, intake/exhaust system, fuel supply, injection system, oxygen/NOx sensor, water coolant system, catalyst, data collection system, and a control system (pressure and temperature control). The engine displacement is 638×10^{-6} m^3 and the piston measures 92 mm in diameter, while the stroke is 96 mm in length. The sub-chamber displacement is 23.5×10^{-6} m^3 and it is connected to the main chamber by a 52.6 mm^2 orifice. The engine has a compression ratio of 17.7, which is almost twice as high as the typical compression ratio of a general SI engine. At the upper part of the sub-chamber, a spark plug was installed using an adapter. An ammonia and gasoline tank are connected to injectors that were installed in the intake port. In the main chamber, a pressure sensor (Kistler 5018A) was installed to measure the change in pressure. The engine is connected to an eddy current dynamometer through an electromagnetic clutch, which is used to adjust the engine speed. The intake pressure is adjusted manually by a throttle valve to maintain constant intake pressure, which is then measured by the intake manifold pressure sensor. The general-purpose ECU (INFINITY SERIES7) is used to control the fuel injection quantity and ratio (NH_3 and gasoline), control the injection timing, control the ignition timing, and receive signals to transmit into the data logger (fuel injection signal, ignition signal, and sensor signal). The rotary encoder (E6B2-CWZ6C) sends a TDC signal to the ECU every two revolutions of the crankshaft, which is used to monitor the location of the piston during the combustion experiment in real time. The HORIBA MEXA-720, which is an oxygen and NO_x (NO/NO_2) sensor, is located in the exhaust pipe to measure the engine emissions. The coolant system is made up of a coolant heater, a heat exchanger, and a pump. The coolant temperature sensor monitors the coolant temperature and sends the data to the ECU. A catalyst and a catalyst heater are installed before the exhaust pipe, these are used to purify the unburned gas in the combustion experiment.

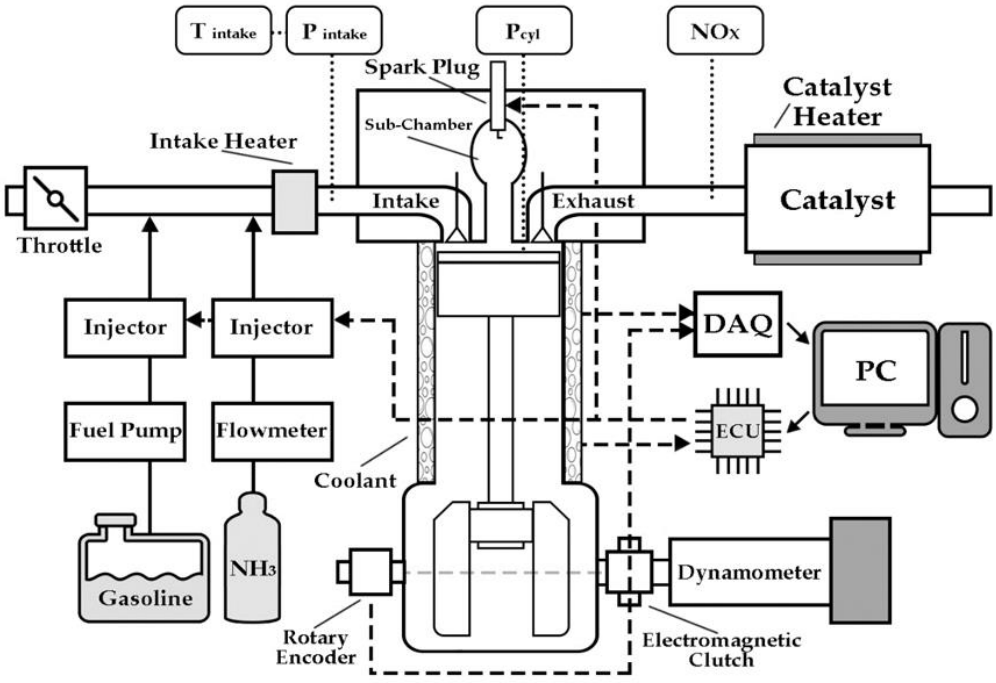

Figure 1. Schematic of the experimental apparatus

Table 1. Engine specifications

Engine model	: YANMAR TF 120V - E
Engine type	: Horizontal single cylinder diesel
Valve mechanism	: Overhead valve
Ignition method	: Spark ignition
Fuel supply	: Port injection
Standard injection timing [CA ATDC]	: -30°
Sub-chamber	: Spherical swirl
Type of aspiration	: Natural aspiration
Bore x stroke [mm]	: 92 x 96
Compression ratio [-]	: 17.7
Total displacement [m^3]	: 638×10^{-6}
Sub-chamber displacement [m^3]	: 23.5×10^{-6}
Max speed [rpm]	: 2400
Cooling system	: Water cooling with heat exchanger
Number of orifices	: 1
Cross-sectional area of orifice [mm^2]	: 52.6

2.2. *Operational Process and Conditions*

In this research, the engine performances and combustion characteristics of ammonia/gasoline mixtures in a SI engine with a sub-chamber were investigated. **Table 2** showed the experimental condition used in this study. The methods used in this study involve injecting gaseous ammonia and liquid gasoline into the intake manifold (port fuel injection) with varied injection timing and fuel mixture ratios. Specifically, injection timings of -55° and -10°CA after top dead center (ATDC), were tested. ATDC refers to the top dead center (TDC) after exhaust stroke. The ECU adjusted the ammonia energy ratio in the fuel mixture based on how much the calorific value of ammonia contributed to the total calorific value. The valve timings for the intake and exhaust are also shown in **Table 2**. The earlier injection timing (-55°CA) was during when the intake valve was closed to let the fuel and air mix well before the intake stroke. Moreover, some of the air-NH_3/gasoline fuel mixture was directed into the sub-chamber during the compression stroke. The spark plug was initiated at 366°CA ATDC which was slightly after the compression stroke. During the power stroke, the spark-ignited air-fuel mixture within

the sub-chamber was directed into the main chamber through the orifice. Simultaneously, the remaining air-fuel mixture inside the main chamber was considered as well-mixed. **Table 3** shows the total supplied energy of the fuel mixture and how much of that energy is contributed by the ammonia. Although commands of injection amount of ammonia and gasoline were issued to the ECU according to the calorific value of the fuel mixture, slight variations in the total supplied energy were observed across all conditions. This variance can be attributed to the inherent limitations in the precision of the equipment used.

2.3. *Analytical Methods*

During a combustion process, heat is generally transferred from inside the cylinder to the cylinder walls by both convection and radiation. However, since the radiation heat transfer in a SI engine is negligible [28], this study will only take into account the convection heat transfer. Thus, the heat transfer from the combustion gas to the cylinder wall for each crank angle, Q_{ht} (θ), can be calculated through Eq. (1).

$$Q_{ht(\theta)} = h_{c(\theta)} A_c (T_{(\theta)} - T_w) \quad (1)$$

where h_c is the convective heat transfer coefficient of gas [kW/m²K], A_c is the area of the combustion chamber [m²], $T_{(\theta)}$ is the in-cylinder temperature at each crank angle, T_w is the mean temperature of the cylinder wall, and θ is the crank angle in degrees [°CA]. The heat transfer coefficient, h_c, is based on the Hohenberg's correlation [29], which is expressed in Eq. (2).

$$h_{c(\theta)} = 1879 P_{(\theta)}^{0.8} T_{(\theta)}^{-0.4} V_{(\theta)}^{-0.06} (\overline{S_p} + c)^{0.8} \quad (2)$$

where $P_{(\theta)}$ and $V_{(\theta)}$ are respectively the in-cylinder pressure [MPa] and volume [m³] at each crank angle, c is a calibration factor of 1.4 as suggested by Hohenberg [29], and $\overline{S_p}$ is the mean piston speed [m/s] which can be calculated using Eq. (3).

$$\overline{S_p} = 2S\frac{n}{60} \quad (3)$$

where S is the piston stroke [m] and n is the engine speed [rpm].

The heat release rate (HRR), Q_{HRR} (θ), can be calculated using Eq. (4).

Table 2. Experimental conditions

Engine [RPM]	: 1000
Fuel [-]	: Ammonia, Gasoline
Ammonia energy ratio [%]	: 40, 50, 60, 70
Injection Timing [°CA ATDC]	: 10, -55
Ignition Timing [°CA ATDC]	: 366
Coolant Temperature [°C]	: 70
Intake Pressure [kPa]	: 99
Intake Air Temperature [°C]	: 25
Excess Air Ratio [-]	: 1.0
Intake Valve Opening (IVO) [°CA ATDC]	: -6
Intake Valve Closing (IVC) [°CA ATDC]	: 215
Exhaust Valve Opening (EVO) [°CA ATDC]	: 502
Exhaust Valve Closing (EVC) [°CA ATDC]	: 7

Table 3. Total supplied energy

Injection Timing [°CA ATDC]	Ammonia Energy Ratio [%]	Total Supplied Energy [kJ]
-55	40	1.8328
	50	1.7986
	60	1.7857
	70	1.7558
10	40	1.8229
	50	1.8084
	60	1.7768
	70	1.7823

$$Q_{HRR(\theta)} = \frac{1}{\kappa - 1}\left(V_{(\theta)}\frac{dP}{d\theta} + \kappa P_{(\theta)}\frac{dV}{d\theta}\right) + Q_{ht} \quad (4)$$

where κ is the specific heat ratio, $\frac{dV}{d\theta}$ is the volume rate of change of both main and sub-chamber with respect to the crank angle [m³], and $\frac{dP}{d\theta}$ is the in-cylinder pressure rate of change [MPa] with respect to the crank angle. The acquired in-cylinder pressure data was used to calculate the indicated mean effective pressure (IMEP). The IMEP can be calculated using Eqs. (5) and (6).

$$IMEP = \frac{1}{V_s} \cdot \oint P dV \quad (5)$$

$$IMEP = \frac{1}{V_s} \cdot \sum_{\theta=0}^{a-1} \frac{P_{(\theta+1)} + P_{(\theta)}}{2} \cdot (V_{(\theta+1)} - V_{(\theta)}) \quad (6)$$

where V_s is the stroke volume [m³] and a is the total number of data in one cycle, which is 720 (total °CA).

The coefficient of variance or COV of the IMEP was also calculated in the study and the combustion was considered stable if the COV(IMEP) was less than 5% [30]. Eq. (7) was used to calculate the COV(IMEP) of the combustion.

$$COV(IMEP) = \frac{\sigma IMEP}{\overline{IMEP}} \cdot 100\% \quad (7)$$

where $\sigma IMEP$ is the standard deviation of IMEP [MPa] and $\overline{IMEP}$ is the average IMEP [MPa].

The combustion duration is defined as Eq. (8).

$$Combustion\ Duration = CA90 - CA10 \quad (8)$$

where CA90 and CA10 are respectively the crank angle at which 90% and 10% of the total heat was released.

The combustion efficiency, η_c, can be calculated using Eq. (9).

$$\eta_C = \frac{\int_{\theta_1}^{\theta_2} Q_{HRR} d\theta}{m_a \cdot H_{ua} + m_g \cdot H_{ug}} \quad (9)$$

where θ_1 represents the crank angle at the onset of fuel chemical energy release [°CA], and θ_2 is the crank angle at which all of the fuel chemical energy is released [°CA]. m_a and m_g are the injected mass [kg] of NH_3 and gasoline, respectively. H_{ua} and H_{ug} stand for the lower calorific values [kJ/kg] for NH_3 and gasoline, which are 18,600 kJ/kg and 42,280 kJ/kg, respectively.

The in-cylinder gas temperature [K] can be calculated using Eq. (10).

$$T_{(\theta)} = \frac{P_{(\theta)} \cdot V_{(\theta)}}{P_{IVC} \cdot V_{IVC}} T_{IVC} \quad (10)$$

where P_{IVC}, V_{IVC}, and T_{IVC} are pressure, volume, and temperature at intake valve closing (IVC).

The normalized mass fraction burned (NMFB) was calculated using Eq. (11) by dividing the instantaneous heat release energies between IVC and exhaust valve opening (EVO) timings from the five different injection timing to the heat release energy obtained from the -55°CA ATDC injection timing at 40% ammonia energy ratio case.

$$NMFB = \frac{\int_{\theta_{IVC}}^{\theta_{EVO}} Q_{HRR} d\theta}{\int_{\theta_{IVC}}^{\theta_{EVO}} Q_{HRR(@40\%;-55°CA)} d\theta} \quad (11)$$

The indicated thermal efficiency, η_i, can be calculated using Eq. (12).

$$\eta_i = \frac{W_i}{m_a \cdot H_{ua} + m_g \cdot H_{ug}} \quad (12)$$

where W_i is the indicated work per cycle [kJ] which can be calculated using Eq. (13)

$$W_i = (W_C + W_P) \cdot 1000 \quad (13)$$

$$W_C = \int_{180°}^{360°} P\, dV \quad (14)$$

$$W_P = \int_{360°}^{540°} P\, dV \quad (15)$$

where W_C and W_P are the compression stroke work [kJ] and expansion (power) stroke work [kJ], respectively.

3. Results and Discussion

Figure 2 shows the in-cylinder pressure graphs for (a) 40%, (b) 50%, (c) 60%, and (d) 70% ammonia energy ratio by calorific value. There are two peaks in this in-cylinder pressure graph due to the implementation of a sub-chamber. The first peak was due to the compression stroke, while the second peak was formed as a result of the combustion in the main chamber. The highest overall peak pressure was achieved by injecting the fuel mixture into the intake manifold earlier at

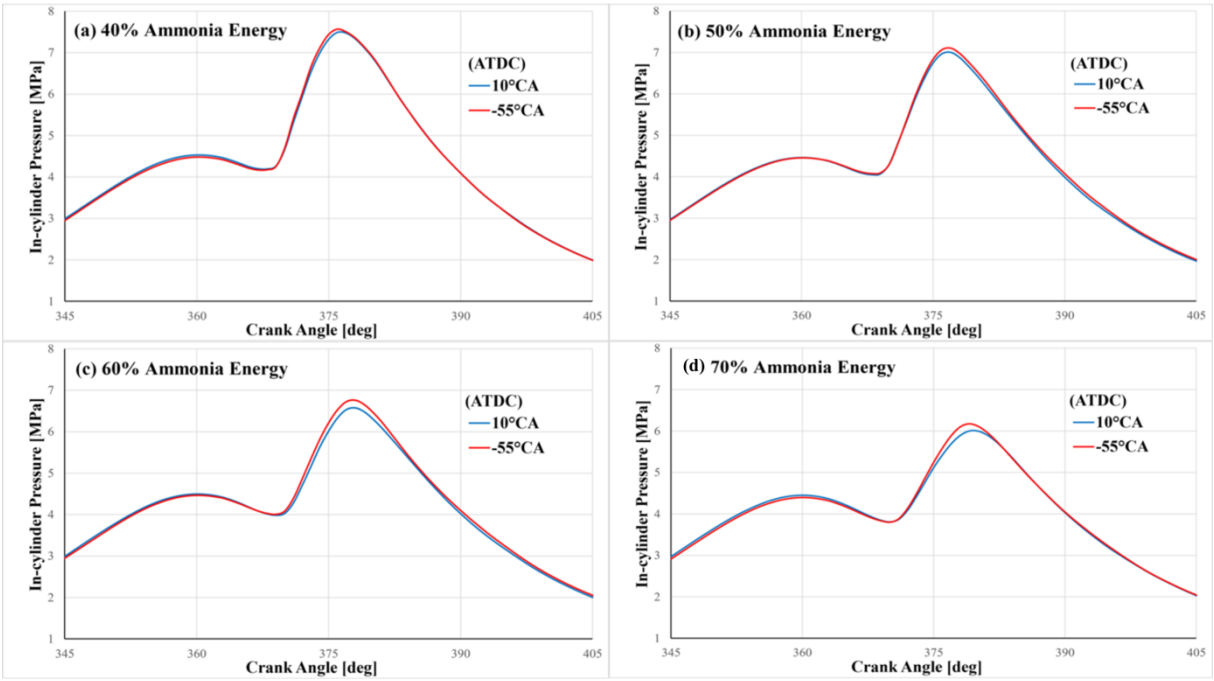

Figure 2. In-cylinder pressure to crank angle degree with different injection timings at (a) 40%; (b) 50%; (c) 60%; (d) 70% ammonia energy ratio

-55°CA ATDC. This implies that advancing the injection timing could facilitate better blending of the air-fuel mixture. On the other hand, increasing the ammonia energy ratio resulted in a downward trend for all the in-cylinder pressure data. This is due to the lower burning capabilities of ammonia [10], [15], [16], thus increasing the proportion of ammonia in the mixture essentially means diluting the fuel mixture with a substance that contributes less to the combustion process. Another noteworthy observation is that both injection timing conditions had similar peak pressure values and achieved those peaks at around the same crank angle degrees. These in-cylinder pressure data was then used to calculate the IMEP and heat release rate under each injection timing condition.

The heat release rate was calculated using Eq. (4) and indicated by **Figure 3a** 40%, **Figure 3b** 50%, **Figure 3c** 60%, and **Figure 3d** 70% ammonia energy ratio. The spark plug was ignited in the sub-chamber at 366°CA, while the main combustion phase was indicated by the central position of the HRR graph, where the bulk of the air-fuel mixture was ignited and burned rapidly, resulting in a significant increase in the heat release rate. At around 375°CA, the majority total fuel mixture was already burned, hence the heat release rate started to drop down. Injection at -55°CA ATDC consistently showed the highest heat release rate when compared to the later injection timing at 10°CA, mostly due to the better mixing of the fuel mixture. Similar to the in-cylinder pressure, increasing the ammonia energy ratio also negatively impacted the heat release rate due to the low flame speed that stemmed from the slow chemical kinetics of NH_3. All conditions then eventually reached an HRR below 0 which implied the existence of cooling lost in the combustion process.

Figure 4 displays the IMEP with different mixture ratios that were calculated using Eq. (6). The general trend for this graph was that the IMEP decreased with higher ammonia energy ratio. This is mainly due to the slow laminar burning velocity characteristic of ammonia. On the other hand, the earlier injection timing allows better premixing between the air and fuel mixture, thus increasing the IMEP of the combustion process. This can be seen as the -55°CA ATDC injection timing consistently produced higher IMEP for 40% to 70% ammonia energy ratio. Using the IMEP data, the COV(IMEP) on **Figure 5** were calculated using Eq. (7) and were found to be lower than 5% for all cases. This implies that all the combustion under different conditions remained relatively stable.

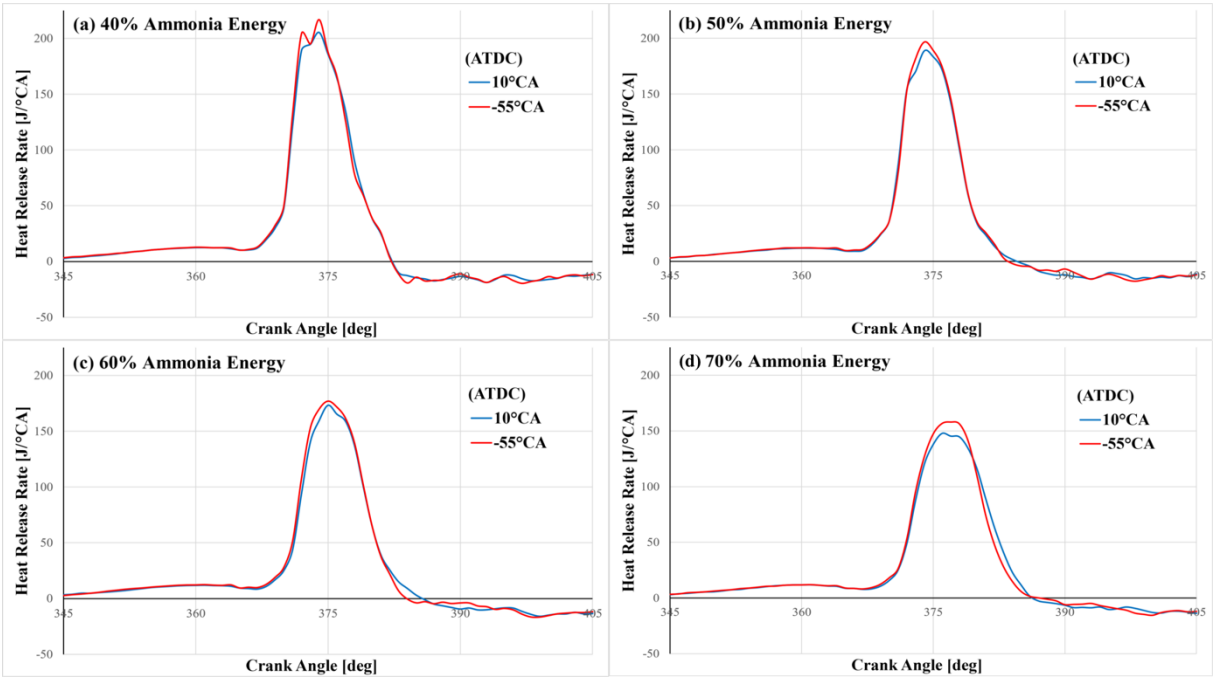

Figure 3. Heat release rate to crank angle degree with different injection timings at (a) 40%; (b) 50%; (c) 60%; (d) 70% ammonia energy ratio

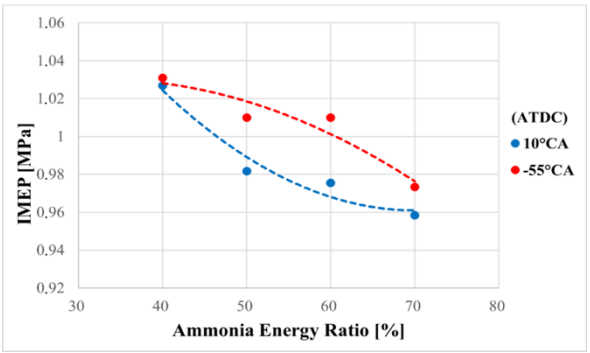

Figure 4. IMEP to ammonia energy ratio with different injection timing conditions

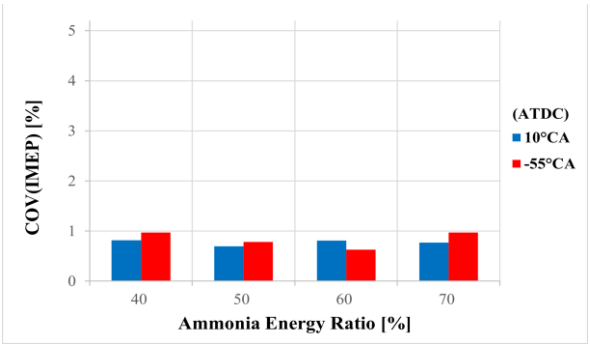

Figure 5. COV(IMEP) to ammonia energy ratio with different injection timing conditions

Figure 6 shows the combustion duration of each condition. As previously stated in section 2, the combustion duration is defined as the crank angle at which 10°CA to 90°CA was achieved. The overall trend was that increasing ammonia energy ratio resulted in longer combustion duration due to the slow burning characteristics of ammonia. At 40% ammonia energy ratio, all combustion durations appeared to have similar values due to gasoline being the majority of the fuel mixture. Both injection timings showed no changes from 40% to 50% ammonia energy ratio. Even though the earlier injection timing of -55°CA ATDC previously performed better for most of the other combustion characteristics, both injection timings achieve the same combustion duration. This may be a result of the limited data collection ability of the research equipment, which can only record data at a 1°CA interval. However, this showed that there was less than 1°CA difference between the two timings, which implies that injection timing is not a significant parameter which affects the combustion duration of the fuel mixture.

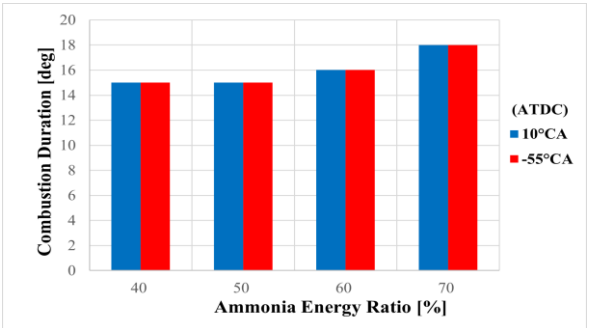

Figure 6. Combustion duration to ammonia energy ratio with different injection timing conditions

Figure 7 shows the overall combustion efficiency with different ammonia energy ratios and injection timings. This efficiency was calculated using Eq. (9). The general trend of the graph shows that increasing the ammonia energy ratio would decrease the combustion efficiency. This is due to the laminar speed and LHV of ammonia being lower than gasoline, which causes a slower energy release from the burned fuel mixture. The -55°CA ATDC injection timing also consistently held the better performance as it was shown to have higher combustion efficiency compared to the retarded injection timing. This is attributed to the better pre-mixing between ammonia and gasoline in the earlier injection timing, which leads to more complete combustion. This can also be seen in the peak gas temperature shown in **Figure 8** which was calculated using Eq. (10). Similar to the previous data, the early injection timing produced a higher peak gas temperature for 40% to 70% ammonia energy ratio. Overall, the graph showed that the peak temperature reduced with the increase in ammonia energy ratio. This is mainly due to the slow combustion effect caused by the reduced gasoline ratio as the ammonia energy ratio increased.

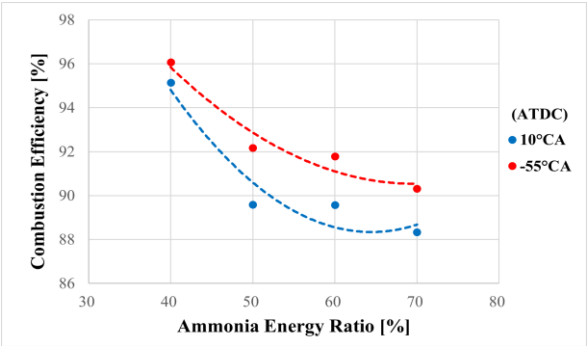

Figure 7. Combustion efficiency to ammonia energy ratio with different injection timing conditions

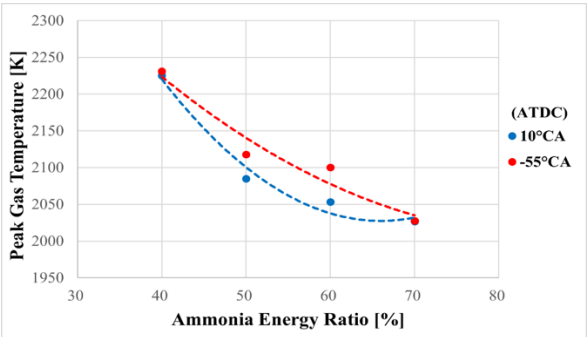

Figure 8. Peak gas temperature to ammonia energy ratio with different injection timing conditions

The increase in ammonia energy ratio reduces the peak temperature as shown in **Figure 8**. Therefore, it is presumed that thermal NOx is also reduced. However, due to the existence of nitrogen in ammonia's molecular structure, NOx emissions were inevitable. **Figure 9** shows the NOx emission with varying ammonia energy ratios. The earlier injection timing at -55°CA ATDC showed an almost linear increasing trend in NOx emissions, while interestingly, the later injection timing at 10°CA ATDC initially showed a rapid increase that proceeded to eventually drop with increasing ammonia energy ratio. The reason for this is due to a process called the denitrification of nitrogen oxides, or DeNOx for short, where the NOx formation is reduced [31]. The shorter mixing time due to the late injection timing and the high ammonia energy ratio created an environment where excess ammonia was present in the combustion chamber, which then reacted to the NOx that was already formed. The resulting products of the following NH_3 and NOx reactions are pure nitrogen and water vapors. In other words, the excess ammonia played a role in NOx removal rather than formation.

Figure 10 shows the normalized mass fraction burned for (a) 40%, (b) 50%, (c) 60%, and (d) 70% ammonia energy ratio under the two injection timings. As shown with the HRR graphs in **Figure 3** where the heat release rate starts to drop down after the 375°CA, it correlates directly with the mass fraction burned where the graph starts to show a concave down shape starting from around 375°CA. This means that the combustion speed of the fuel mixture started to slow down, mostly due to the majority of the fuel being already burned. In line with what was shown in **Figure 6**, due to the slow burning velocity of ammonia, the increase in the ammonia energy ratio resulted in

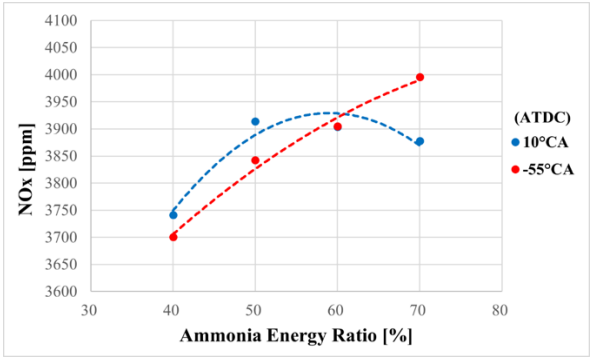

Figure 9. NOx emissions to ammonia energy ratio with different injection timing conditions

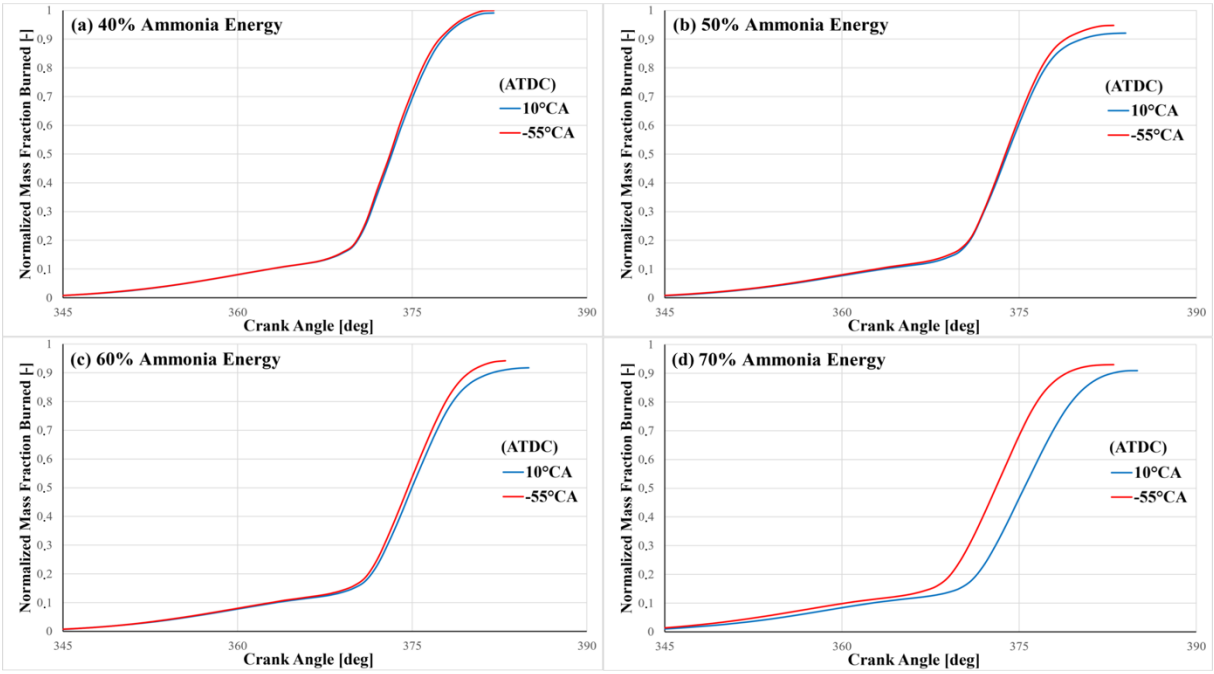

Figure 10. Normalized mass fraction burned to crank angle degree with different injection timings at (a) 40%; (b) 50%; (c) 60%; (d) 70% ammonia energy ratio

an overall wider combustion duration. -55°CA ATDC injection timing showed the highest mass fraction burned regardless of the fuel ratios. This is mainly due to the fuel mixtures and air not having enough time to mix properly at the later injection timing which leads to more unburned fuel during combustion.

Figure 11 shows the indicated thermal efficiency at different ammonia energy ratios with both injection timings. The indicated thermal efficiency was calculated using Eq. (12). A noteworthy observation is that, although the figure shows a downward trend in the indicated thermal efficiency, there is an increase in indicated thermal efficiency from 50% to 60% ammonia energy ratio consistently regardless of the injection timing. This increase in the indicated thermal efficiency is attributed to the IMEP shown in **Figure 4** which shows comparable results at 50% and 60% ammonia energy ratio, while at the same ammonia energy ratio, the energy supply decreases as shown in **Table 3**. Since the IMEP is proportional to the indicated work, the overall efficiency increases due to the lower energy supply. Furthermore, increasing the ammonia energy ratio also reduces the combustion gas temperature which inevitably leads to lower heat losses. Some inconsistencies are present in the graph because the denominator part of the indicated thermal efficiency equation in Eq. (12) is

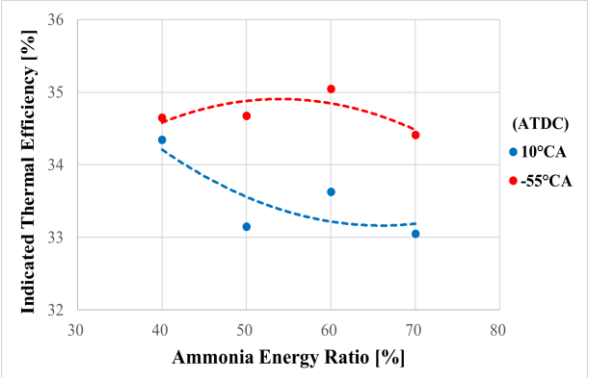

Figure 11. Indicated thermal efficiency to ammonia energy ratio with different injection timing conditions

the theoretical energy supply, while the numerator is the indicated work. Since the combustion in this study utilized a dual fuel mixture, it is extremely difficult to maintain the actual energy supply to the theoretical one, especially with the two components of the fuel mixture having vastly different combustion characteristics.

4. Conclusion

To further investigate the effects of early and late injection timing across 40% to 70% ammonia energy ratio, this study was performed using a modified engine equipped with a sub-chamber that utilized ammonia/gasoline fuel mixtures. As a result, we obtained the following knowledge:

a. For all the tested fuel mixture ratios, the earlier injection timing showed a higher in-cylinder pressure and heat release rate. The HRR values that reached below 0 also confirmed the existence of cooling loss. Furthermore, -55°CA ATDC injection timing also produced an overall better performance in the tested parameters compared to their retarded counterpart. This can be attributed to the better premixing between the air and fuel mixture with earlier injection timing.
b. The stability of the combustion was tested by calculating the COV(IMEP) and it was found that the combustion was relatively stable for all injection timings as none of the COV(IMEP) reached above 5%.
c. While the -55°CA ATDC injection timing outperformed their retarded counterpart in various other combustion characteristics, both injection timings produced a similar combustion duration. This suggests that the injection timing is not a major factor influencing the combustion duration of the fuel mixture.
d. The injection timing occurring before TDC at -55°CA exhibited a semi-constant rising pattern in NOx emissions, whereas the injection timing taking place after TDC at 10°CA demonstrated a rapid increase that slowed down with increasing ammonia energy ratio. The reason was due to the DeNOx process caused by the shorter mixing time and the higher ammonia energy ratio that mitigates the NOx formation.
e. With increased ammonia energy ratio, IMEP, combustion efficiency, and peak gas temperature decreased, and the combustion duration becomes longer. This can be attributed to the difficulty to combust ammonia since the supplied energy content between different ammonia energy ratios are similar.
f. The indicated thermal efficiency showed an increase from 50% to 60% ammonia energy ratio due to their comparable IMEP, and since the IMEP is proportional to the indicated work, the decrease in energy supply results in an overall boost to the indicated thermal efficiency.

Acknowledgements

The research was supported by Sophia University, Japan and Petra Christian University, Indonesia in an international collaborative project. The authors are grateful to the two institutions for their support.

Author's Declaration

Authors' contributions and responsibilities

The authors made substantial contributions to the conception and design of the study. The authors took responsibility for data analysis, interpretation and discussion of results. The authors read and approved the final manuscript.

Funding

This work was supported by the Japan Society for the Promotion of Science, Grants-in-Aid for Scientific Research (No. 19K04244), Sophia University Special Grant for Academic Research, Research in Priority Areas, and Petra Christian University (Project code: 097/PSTM/ST/2023).

Availability of data and materials

All data are available from the authors.

Competing interests

The authors declare no competing interest.

Additional information

No additional information from the authors.

References

[1] United States Environmental Protection Agency, "Global Greenhouse Gas Emissions Data," *Environmental Protection Agency*, 2023.

[2] Our World in Data, "Fossil Fuels," *Our World in Data*, 2023.

[3] A. M. Zope, R. K. Swami, and A. Patil, "SEM Approach for Analysis of Lean Six Sigma Barriers to Electric Vehicle Assembly," *Automotive Experiences*, vol. 6, no. 2, pp. 416–428, Aug. 2023, doi: 10.31603/ae.9690.

[4] Y. D. Herlambang *et al.*, "Study on Solar Powered Electric Vehicle with Thermal Management Systems on the Electrical Device Performance," *Automotive Experiences*, vol. 7, no. 1, pp. 18–27, 2024, doi: 10.31603/ae.10506.

[5] H. Maghfiroh, O. Wahyunggoro, and A. I. Cahyadi, "Low Pass Filter as Energy Management for Hybrid Energy Storage of Electric Vehicle: A Survey," *Automotive Experiences*, vol. 6, no. 3, pp. 466–484, 2023,

doi: 10.31603/ae.9398.

[6] M. Aziz, A. T. Wijayanta, and A. B. D. Nandiyanto, "Ammonia as Effective Hydrogen Storage: A Review on Production, Storage and Utilization," *Energies*, vol. 13, no. 12, p. 3062, Jun. 2020, doi: 10.3390/en13123062.

[7] M. Wahyu, H. Rahmad, and G. J. Gotama, "Effect of Cassava Biogasoline on Fuel Consumption and CO Exhaust Emissions," *Automotive Experiences*, vol. 2, no. 3, pp. 97–103, 2019, doi: 10.31603/ae.v2i3.2991.

[8] E. Marlina, M. Basjir, M. Ichiyanagi, T. Suzuki, G. J. Gotama, and W. Anggono, "The Role of Eucalyptus Oil in Crude Palm Oil As Biodiesel Fuel," *Automotive Experiences*, vol. 3, no. 1, pp. 33–38, 2020, doi: 10.31603/ae.v3i1.3257.

[9] S. Sunaryo, S. Suyitno, Z. Arifin, and M. Setiyo, "Performance and emission of a spark-ignition engine using gasoline-plastic pyrolysis oil blends," *Mechanical Engineering for Society and Industry*, vol. 4, no. 1, pp. 68–81, Jul. 2024, doi: 10.31603/MESI.11278.

[10] A. Hayakawa, T. Goto, R. Mimoto, Y. Arakawa, T. Kudo, and H. Kobayashi, "Laminar burning velocity and Markstein length of ammonia/air premixed flames at various pressures," *Fuel*, vol. 159, pp. 98–106, Nov. 2015, doi: 10.1016/j.fuel.2015.06.070.

[11] M. Setiyo, "Alternative fuels for transportation sector in Indonesia," *Mechanical Engineering for Society and Industry*, vol. 2, no. 1, pp. 1–6, 2022, doi: 10.31603/mesi.6850.

[12] E. Rivard, M. Trudeau, and K. Zaghib, "Hydrogen Storage for Mobility: A Review," *Materials*, vol. 12, no. 12, p. 1973, Jun. 2019, doi: 10.3390/ma12121973.

[13] M. Koike, H. Miyagawa, T. Suzuoki, and K. Ogasawara, "Ammonia as a hydrogen energy carrier and its application to internal combustion engines," *Sustainable Vehicle Technologies*, pp. 61–70, 2012, doi: 10.1533/9780857094575.2.61.

[14] D. Lanni, E. Galloni, G. Fontana, and G. D'Antuono, "Assessment of the Operation of an SI Engine Fueled with Ammonia," *Energies*, vol. 15, no. 22, p. 8583, Nov. 2022, doi: 10.3390/en15228583.

[15] V. F. Zakaznov, L. A. Kursheva, and Z. I. Fedina, "Determination of normal flame velocity and critical diameter of flame extinction in ammonia-air mixture," *Combustion, Explosion, and Shock Waves*, vol. 14, no. 6, pp. 710–713, Nov. 1978, doi: 10.1007/BF00786097.

[16] K. Takizawa, A. Takahashi, K. Tokuhashi, S. Kondo, and A. Sekiya, "Burning velocity measurements of nitrogen-containing compounds," *Journal of Hazardous Materials*, vol. 155, no. 1–2, pp. 144–152, Jun. 2008, doi: 10.1016/j.jhazmat.2007.11.089.

[17] T. McSweeney and J. Holbrook, "Ammonia Safety," 2006.

[18] M. Sakai, M. Kiya, T. Irie, and H. Yakuwa, "Study of Stress Corrosion Cracking Test Method for Pure Copper Tube in Ammoniacal Environment," *Zairyo-to-Kankyo*, vol. 65, no. 4, pp. 138–142, 2016, doi: 10.3323/jcorr.65.138.

[19] E. Yilmaz *et al.*, "Investigation of intake air temperature effect on co-combustion characteristics of NH3/gasoline in naturally aspirated high compression ratio engine with sub-chamber," *Scientific Reports*, vol. 13, no. 1, p. 11649, Jul. 2023, doi: 10.1038/s41598-023-38883-3.

[20] E. C. Okafor *et al.*, "Measurement and modelling of the laminar burning velocity of methane-ammonia-air flames at high pressures using a reduced reaction mechanism," *Combustion and Flame*, vol. 204, pp. 162–175, Jun. 2019, doi: 10.1016/j.combustflame.2019.03.008.

[21] G. J. Gotama *et al.*, "Measurement of the laminar burning velocity and kinetics study of the importance of the hydrogen recovery mechanism of ammonia/hydrogen/air premixed flames," *Combustion and Flame*, vol. 236, p. 111753, Feb. 2022, doi: 10.1016/j.combustflame.2021.111753.

[22] Y. Zhang, W. Zhou, Y. Liang, L. Yu, and X. Lu, "An experimental and detailed kinetic modeling study of the auto-ignition of NH3/diesel mixtures: Part 1- NH3 substitution ratio from 20% to 90%," *Combustion and Flame*, vol. 251, p. 112391, May 2023, doi:

10.1016/j.combustflame.2022.112391.

[23] L. Dai *et al.*, "Ignition delay times of NH3 /DME blends at high pressure and low DME fraction: RCM experiments and simulations," *Combustion and Flame*, vol. 227, pp. 120–134, May 2021, doi: 10.1016/j.combustflame.2020.12.048.

[24] B. Guo *et al.*, "Combustion Analysis of Ammonia Fueled High Compression Ratio SI Engine with Glow Plug and Sub-Chamber," *International Journal of Automotive Engineering*, vol. 13, no. 1, p. 20224073, 2022, doi: 10.20485/jsaeijae.13.1_1.

[25] W. Anggono *et al.*, "Engine Performances of Lean Iso-Octane Mixtures in a Glow Plug Heated Sub-Chamber SI Engine," *Automotive Experiences*, vol. 5, no. 1, pp. 16–27, Nov. 2021, doi: 10.31603/ae.5118.

[26] C. Mounaïm-Rousselle, A. Mercier, P. Brequigny, C. Dumand, J. Bouriot, and S. Houillé, "Performance of ammonia fuel in a spark assisted compression Ignition engine," *International Journal of Engine Research*, vol. 23, no. 5, pp. 781–792, May 2022, doi: 10.1177/14680874211038726.

[27] T. Nguyen and T. Hoang, "Effects of ethanol port injection timing and delivery rate on combustion characteristic of a heavy-duty V-12 diesel engine," *Thermal Science*, vol. 26, no. 1 Part A, pp. 343–352, 2022, doi: 10.2298/TSCI200710137N.

[28] M. S. Lounici, K. Loubar, M. Balistrou, and M. Tazerout, "Investigation on heat transfer evaluation for a more efficient two-zone combustion model in the case of natural gas SI engines," *Applied Thermal Engineering*, vol. 31, no. 2–3, pp. 319–328, Feb. 2011, doi: 10.1016/j.applthermaleng.2010.09.012.

[29] G. F. Hohenberg, "Advanced Approaches for Heat Transfer Calculations," Feb. 1979, doi: 10.4271/790825.

[30] L. Wang *et al.*, "Experimental study on the high load extension of PODE/methanol RCCI combustion mode with optimized injection strategy," *Fuel*, vol. 314, p. 122726, Apr. 2022, doi: 10.1016/j.fuel.2021.122726.

[31] R. Lyon, "The Chemistry of the Thermal DeNOx Process: A Review of the Technology's Possible Application to control of NOx from Diesel Engines," University of North Texas, 2001.